Dynamic GNNs for Precise Seizure Detection and Classification from EEG Data

Arash Hajisafi[1][0009−0000−1056−0640], Haowen Lin[1][0000−0002−4097−1907], Yao-Yi Chiang[2][0000−0002−8923−0130], and Cyrus Shahabi[1][0000−0001−9118−0681]

[1] University of Southern California, Los Angeles, CA, USA
{hajisafi,haowenli,shahabi}@usc.edu
[2] University of Minnesota, Minneapolis, MN, USA yaoyi@umn.edu

Abstract. Diagnosing epilepsy requires accurate seizure detection and classification, but traditional manual EEG signal analysis is resource-intensive. Meanwhile, automated algorithms often overlook EEG's geometric and semantic properties critical for interpreting brain activity. This paper introduces NeuroGNN, a dynamic Graph Neural Network (GNN) framework that captures the dynamic interplay between the EEG electrode locations and the semantics of their corresponding brain regions. The specific brain region where an electrode is placed critically shapes the nature of captured EEG signals. Each brain region governs distinct cognitive functions, emotions, and sensory processing, influencing both the semantic and spatial relationships within the EEG data. Understanding and modeling these intricate brain relationships are essential for accurate and meaningful insights into brain activity. This is precisely where the proposed NeuroGNN framework excels by dynamically constructing a graph that encapsulates these evolving spatial, temporal, semantic, and taxonomic correlations to improve precision in seizure detection and classification. Our extensive experiments with real-world data demonstrate that NeuroGNN significantly outperforms existing state-of-the-art models.

Keywords: Dynamic Graph Neural Network (GNN) · Automated Seizure Detection & Classification · EEG Data Analysis.

1 Introduction

Seizure detection and classification from EEG data is crucial for diagnosing epilepsy, a neurological disorder affecting around 1% of the global population, with classification being particularly important for precise treatment [6]. The conventional approach to seizure detection and classification is largely manual, requiring skilled personnel to analyze extensive EEG recordings. This manual process is time-consuming, expensive, and prone to human errors [11,30].

Automated approaches using Convolutional Neural Networks (CNNs) [26] and Recurrent Neural Networks (RNNs) [21] have been explored to tackle these

challenges. However, these architectures do not capture the relationships between EEG observations in various brain regions, a crucial aspect of understanding the underlying neurological dynamics during seizures. Graph Neural Networks (GNNs) can capture relationships among EEG data points using a graph representation, yet existing GNN-based approaches either rely on predefined relations to generate a static graph or only use temporal correlations for dynamic graph generation, overlooking spatial and semantic relationships [8,30]. Such approaches miss out on leveraging multiple informative contexts and often result in poor performance, especially in scenarios marked by data scarcity, such as in classifying rare seizure types. Toward this end, a comprehensive solution is needed to automatically capture both static and dynamic evolving relationships and incorporate temporal, spatial, and semantic contexts simultaneously. This would allow for a detailed representation of the underlying correlations within the brain, enabling an end-to-end methodology for seizure detection and classification while overcoming the limitations of training under data scarcity.

Drawing inspiration from BysGNN [8], a GNN framework that creates a dynamic multi-context graph for forecasting visits to points of interest (POIs) based on spatial, temporal, semantic, and taxonomic contexts, we aim to generate a similar multi-context graph for our EEG data. However, adapting BysGNN as is to our domain presents several challenges. First, the shift from time-series forecasting in BysGNN to a multivariate time-series classification task in our work requires a change in architectural design. While BysGNN focuses on patterns within individual graph entities for node regression, our goal requires learning broader patterns across entities to perform graph classification. Second, EEG signals represent neurological events, which causes the translation of multi-context correlations from the POI domain to EEG data to be complex due to the underlying neurological mechanisms in brain activity and functional dependencies. Specifically, this translation is nontrivial because (1) the semantic contexts and relationships in brain areas are based on the functional roles of the corresponding part of the brain or broader brain region, which differs from the semantics of POI visits; (2) unlike POI's geographical coordinates, spatial contexts in EEG data are based on the brain's anatomy and EEG electrode placements; (3) the higher-level patterns in the brain should be defined based on the field of neuroscience, which is not as straightforward as defining high-level visit patterns to POIs. Finally, there are far fewer training samples for seizure classification, especially for rare seizure types, which necessitates designing a pretraining strategy aligned with the multi-context correlation notion to achieve optimal seizure detection and classification performance.

To address these challenges, we propose NeuroGNN, a GNN-based framework designed to dynamically construct a graph encapsulating multi-context correlations in EEG data. The correlations are characterized by spatial proximity of electrode placements on the scalp, temporal dependencies within and between time series from different electrodes, semantic similarities derived from neurological brain functions of respective electrode placements, and taxonomic correlations across broader brain regions. The broader regions are defined through

neuroscientific meta-nodes generated from EEG electrodes, extending the multi-context definitions to these meta-nodes. Our new design incorporates hierarchical pooling to handle node and meta-node representations and employs Bidirectional Gated Recurrent Units (BiGRUs) to enhance the intra-series capture and characterization of time-series data. To address the challenge of small training samples and achieve optimal performance across both detection and classification, we develop a new pretraining strategy with a learning objective that aligns with our graph representation, encompassing both nodes and meta-nodes. Learning to generate this multi-context graph representation allows NeuroGNN to outperform state-of-the-art methods for seizure detection and classification in real-world EEG diagnosis scenarios. Through comprehensive ablation studies, we demonstrate that each multi-context correlation modality significantly contributes to the overall performance enhancement. This is particularly noticeable in rare classes with training under data scarcity.

2 Related Work

EEG signals are commonly used to detect epileptic seizures (e.g., [26]). Since manual EEG analysis by trained physicians is extremely resource and time-intensive, much recent research has focused on using machine learning approaches to automate the diagnostic process. Diagnosing epileptic seizures can be divided into seizure detection and seizure classification. Seizure detection aims to detect abnormal patterns in EEG data. Initially, for seizure detection, researchers started with conventional machine learning techniques, where they first extracted hand-engineered frequency features from the recordings and applied traditional methods such as K-Nearest Neighbors and random forests to detect abnormal EEG signals [16]. Shortly afterward, Roy et al. suggested employing time-distributed neural networks, such as recurrent neural networks, to learn directly from the data without any explicit pre-processing step [21]. Sharathappriyaa et al. propose to compress EEG signals into a latent space representation using Autoencoders and then detect epileptic seizures [25].

Seizure classification differentiates between seizure types like focal or generalized seizures. Most of the works in seizure classification adopt CNNs for EEG-based seizure prediction [26]. For example, Bhattacharyya et al. first transform the 1D signal of each EEG channel into 2D using wavelet transform and then apply a CNN to detect and classify seizure subtypes [4]. However, CNN-based methods often overlook the complex spatial structures of EEG sensors and brain geometry [30]. To address this, recent efforts have explored graph-based neural networks, which better capture these spatial relationships, achieving enhanced detection and classification results [30]. Yet, existing GNN studies on EEG data present a significant limitation: they either assume a static graph structure based solely on EEG sensor distances or generate dynamic graphs considering only the temporal relationships between EEG. Both approaches are constrained, representing only a single type of relationship in the graph structure, spatial or temporal, and thus fail to fully capture the complex interactions among EEG sensors
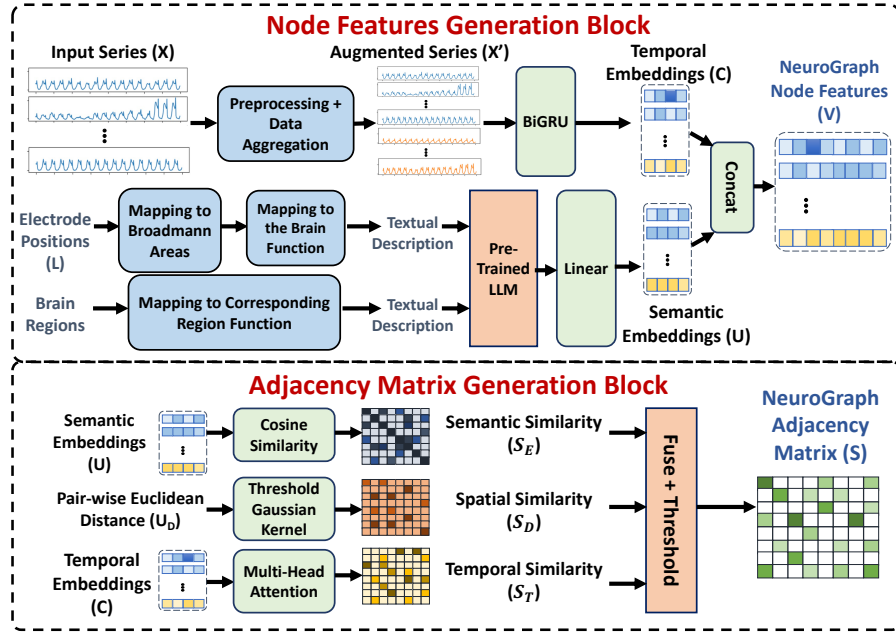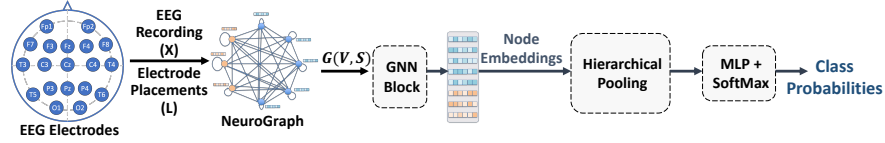
Fig. 1: **NeuroGNN Graph Construction**

Fig. 2: **Seizure Detection and Classification using NeuroGraph**

and their signals. Our model addresses this gap by effectively fusing complex relationships from multiple dimensions to create dynamic graphs that improve automatic seizure detection and classification.

3 Methodology: NeuroGNN

Given EEG recordings within a time-series window X and the 3D coordinates L of electrode placements on the scalp, we first construct the dynamic Neuro-Graph G, integrating multi-context relations, as illustrated in Figure 1. This graph's nodes encapsulate current temporal EEG data and corresponding brain semantics. Edges fuse spatial, temporal, and semantic information to model complex inter-node relationships. Subsequently, as depicted in Figure 2, the GNN block updates the node embeddings, leveraging these multi-contextual edges. Hierarchical pooling aggregates these embeddings into a single graph-level vector, which is then classified via an MLP, enabling both binary classification for seizure detection and multi-label classification for seizure type prediction. Detailed procedures are in subsequent sections.

3.1   Node Features Generation

The process begins by preprocessing the time-series data and generating new aggregated series to form six meta-nodes, each representing a distinct brain region as identified in [1]. These meta-nodes, representing regional neural activities, complement EEG nodes that capture only localized activities, facilitating a multi-scale representation for learning taxonomic correlations. Meta-nodes aggregate EEG data within their regions through an averaging function on the input $\mathbf{X} \in \mathbb{R}^{N \times T}$, producing $X' \in \mathbb{R}^{N' \times T}$ where $N' = N + 6$ (representing the addition of six brain regions).

Next, to capture intra-series temporal correlations, X' is fed into a Bidirectional Gated Recurrent Unit (BiGRU) [12]. BiGRU's bidirectional processing provides a comprehensive representation of the given time-series window, which is crucial for seizure detection and classification. The BiGRU generates hidden states for each node, denoted as $h_{f,i} \in \mathbb{R}^M$, representing forward temporal dynamics and $h_{b,i} \in \mathbb{R}^M$, representing backward temporal dynamics from the forward and backward passes, respectively, where M shows the hidden dimension. The final node embedding is obtained by concatenating the two hidden states, $c_i = (h_{f,i} \parallel h_{b,i})$, forming an embedding matrix $C \in \mathbb{R}^{N' \times 2M}$.

In parallel, NeuroGNN captures semantic correlations among EEG nodes and meta-nodes using a pre-trained Large Language Model (LLM). The semantic foundations are based on Brodmann areas, which segment the cerebral cortex into distinct functional regions [33]. A mapping between EEG electrode placements L and Brodmann areas is established as per [23]. Textual descriptions encapsulating the functional roles of the corresponding Broadmann areas and brain regions are generated for each EEG node and meta-node based on reputable scientific resources [29,33]. These descriptions are tokenized and fed into a pre-trained MPNet language model [28], which is fine-tuned via a linear layer during training to optimize semantic embeddings for the downstream task, resulting in a semantic embeddings matrix $U \in \mathbb{R}^{N' \times K}$, where K denotes the semantic embedding dimensionality.

The final feature vector for each node and meta-node is obtained by concatenating the temporal and semantic embeddings, yielding the NeuroGraph node features matrix $V \in \mathbb{R}^{N' \times (2M+K)}$.

3.2   Adjacency Matrix Generation

Next, we construct NeuroGraph's adjacency matrix to dynamically capture multi-context correlations among EEG and meta-nodes.

First, we compute the semantic similarity matrix S_E using cosine distance on semantic embeddings from the node features generation layer. In parallel, we compute spatial and temporal similarities. Spatial similarities are derived by first calculating Euclidean distances among EEG electrodes for EEG node pairs, and average distance for meta-node pairs and meta-node to EEG node pairs. The spatial similarity matrix S_D is then formed by applying a Gaussian kernel [27] to convert distance metrics into similarity scores, controlled by a threshold τ. Temporal similarities are captured by passing temporal embeddings C to a Multi-Head Attention layer [31], resulting in a temporal similarity matrix S_T.

To fuse these similarities, we employ a gating mechanism, $S_{Gate} = (1-\alpha)S_E + \alpha S_D$ to control influence of temporal similarities, forming an un-thresholded adjacency matrix $S' = S_{Gate} \odot S_T$, with α as a learnable parameter between 0 and 1 to adjust the balance between the importance of spatial and semantic similarities. A thresholding step [8] refines S' to obtain the final adjacency matrix S, retaining reliable similarity scores and discarding noisy ones.

3.3   Prediction using the Generated NeuroGraph

With the generated node features V and adjacency matrix S, the NeuroGraph $G = (V, S)$ for a given window is formed, encapsulating multi-context relationships among EEG nodes and meta-nodes. NeuroGraph is then passed through a GNN block employing a modified Graph Convolutional Networks (GCN) variant [14], omitting the normalization term and adding residual connections between the message passing layers, to preserve directed relationships in NeuroGraph and mitigate oversmoothing [5], respectively. This yields the node embeddings matrix $V' \in \mathbb{R}^{N' \times Z}$, where Z represents the embedding dimension.

Next, a hierarchical pooling mechanism aggregates refined node representations into a single graph embedding vector. Initially, within each brain region, a max-pooling operation aggregates EEG node embeddings. Similarly, a max-pooling operation across all meta-nodes constructs a single embedding vector for meta-nodes. These pooled embeddings are concatenated, forming a collective representation of region-wise and meta-wise node information. A feature-wise mean-pooling operation on this concatenated representation derives the graph embedding vector $\mathbf{g} \in \mathbb{R}^Z$, encapsulating critical graph information.

Finally, vector $\mathbf{g}$ is processed through a Multi-Layer Perceptron (MLP) with a Softmax activation to obtain the final class probabilities. For training detection and classification models, binary and multi-class cross-entropy are utilized as loss functions, respectively.

3.4   Pretraining

Pretraining can mitigate issues related to the scarcity of labeled data and out-of-distribution predictions in many scientific ML applications [32,9]. Therefore, we assess NeuroGNN's performance with weights initialized after a pretraining phase on a self-supervised task. The chosen pretraining task is a node-level regression task, which forecasts future values for the upcoming 12 seconds from a 60s preprocessed EEG clip for each EEG node and meta-node. We design two training objectives; **Primary Objective:** Minimizing Forecasting Mean Squared Error (MSE) Loss across all EEG nodes and meta-nodes, and **Secondary Objective:** Ensuring Consistency Loss to maintain forecast consistency between individual nodes and their corresponding meta-nodes. The overall training objective combines both objectives with a weighted sum.

Table 1: Summary of TUSZ v1.5.2 used in our study

Set	EEG Files		Total Seizure Duration		Patients		CF Seizures		GN Seizures		AB Seizures		CT Seizures	
	Non-Seizure	Seizure	Non-Seizure	Seizure	Non-Seizure	Seizure	Seizures	Patients	Seizures	Patients	Seizures	Patients	Seizures	Patients
Train Set	3730	869	705h 29m	47h 26m	390	202	1,868	148	409	68	50	7	48	11
Test Set	670	230	135h 46m	14h 45m	10	35	297	24	114	11	49	5	61	4

4 Experiments

4.1 Experimental Setup

Dataset and Data Splits We conducted our experiments using the Temple University Hospital EEG Seizure Corpus (TUSZ) v1.5.2 [24,20]. The dataset comprises $3,050$ annotated seizure events from over 300 patients across eight seizure types, with data recorded using 19 electrodes from the standard 10-20 EEG system. We follow [30] to preprocess and group the seizures into four classes. Table 1 details the statistics of the data used in our experiments. The training set was randomly split into training and validation sets with a 9:1 ratio.

Preprocessing Following prior methodologies [30,2,3], EEG recordings were resampled to 200Hz and divided into 60-second non-overlapping windows (clips). For seizure detection, all EEG clips are utilized; a clip is labeled as a seizure if it contains at least one type of seizure. For seizure classification, only clips with a single seizure type are used. If a seizure ends and another begins within a clip, it is truncated and zero-padded to maintain a 60-second length. Each 60-second clip is further divided into 1-second segments, with the Fast Fourier Transform (FFT) applied to each segment to obtain log amplitudes of non-negative frequency components, as per [30]. Each 60-second clip, now a sequence of 60 log-amplitude representations, is used for classification.

Training Training was conducted on a RTX 3090 GPU with 24GB of memory under an Ubuntu 20.04 setup with CUDA version 11.4, and PyTorch v1.13.0. Without pretraining, model weights were initialized using the Xavier initialization method [7]. The Adam optimizer [13] was utilized for training, paired with a cosine annealing learning rate scheduler [17]. The training was continued until the evaluation loss increased in 5 consecutive epochs or reached a maximum of 100 epochs. $L2$ regularization was applied to model weights to prevent overfitting. In seizure detection and classification, the model checkpoint achieving the best Area Under the Receiver Operating Characteristic (AUROC) and weighted F1 score on the validation set across different epochs were preserved, respectively. The pretraining task also ran for 300 epochs. The obtained weights for Node Features Generation, Adjacency Matrix Generation, and GNN Block parameters then initialized the model for the following downstream task.

Baselines We benchmarked NeuroGNN against: (1) **LSTM** [10], for encoding sequential data; (2) **Dense-CNN** [22] that used a densely connected architecture for seizure detection; (3) **CNN-LSTM** [2] integrated 2D convolutions with LSTM for seizure classification; (4) **Corr-DCRNN** [30], a GNN-based model that utilized the DCRNN [15] framework on graphs formed from EEG data cross-correlation at each timestep; and (5) **Dist-DCRNN** [30], another GNN variant leveraging DCRNN on a graph constructed from Euclidean distances of EEG electrode placements. The latter two represent current state-of-the-art (SOTA) in this domain.

Table 2: Experiment results. The highest and second highest scores are denoted in bold and italics with underline, respectively. "Improvement" shows the percentage improvement of NeuroGNN compared to the best-performing baseline. The mean and standard deviations are from three random runs.

Method	Seizure Detection (AUROC)		Seizure Classification (Weighted F1)	
	Without Pretraining	With Pretraining	Without Pretraining	With Pretraining
LSTM	0.715 ± 0.016	–	0.686 ± 0.020	–
Dense-CNN	0.796 ± 0.014	–	0.626 ± 0.073	–
CNN-LSTM	0.682 ± 0.003	–	0.641 ± 0.019	–
Corr-DCRNN	$\underline{0.804 \pm 0.015}$	0.850 ± 0.014	$\underline{0.701 \pm 0.030}$	$\underline{0.749 \pm 0.017}$
Dist-DCRNN	0.793 ± 0.022	$\underline{0.875 \pm 0.016}$	0.690 ± 0.035	$\underline{0.749 \pm 0.028}$
NeuroGNN	$\mathbf{0.847 \pm 0.007}$	$\mathbf{0.876 \pm 0.002}$	$\mathbf{0.790 \pm 0.006}$	$\mathbf{0.792 \pm 0.004}$
Improvement	+5.35%	+0.11%	+12.7%	+5.74%

Hyperparameter Setting Cross-validation was used to select hyperparameters for optimal performance. Key settings include an initial learning rate of 0.0002, batch size of 40, hidden BiGRU dimension M and semantics embedding dimension K both at 512. Multi-Head Attention utilized 8 heads, while graph convolution node embedding dimension Z was set to 256. Gaussian kernel threshold τ was set to twice the standard deviation of EEG electrode distances. For pretraining, the MSE loss objective weight was set to 0.9, and the Consistency loss objective weight was adjusted to 0.1. These settings were consistent across both detection and classification tasks.

4.2   Results

NeuroGNN Performance Table 2 presents the results using the evaluation metrics following convention [30,3,18,2]. NeuroGNN outperforms baseline models in seizure detection and classification in both pretraining scenarios. In seizure detection, non-pretrained Corr-DCRNN shows a slight 1.01% improvement over Dense-CNN, while NeuroGNN boosts the AUROC score by over 5% compared to SOTA Corr-DCRNN, underscoring the benefits of capturing multi-context correlations. Both Dist-DCRNN and Corr-DCRNN, tackling different correlation aspects, spatial and temporal, individually, yield similar performance on both tasks. Conversely, NeuroGNN, integrating multi-context correlations within a unified framework, shows substantial performance improvement against DCRNN-based baselines. Particularly in classification, NeuroGNN significantly improves the weighted F1 score of DCRNN-based baselines by 12.7% without pretraining and by 5.74% after pretraining, respectively.

The improvement in seizure detection achieved by NeuroGNN over baselines, while noteworthy, is less significant compared to the enhancement in seizure classification performance. This difference can be attributed to the binary nature of the detection task and the abundance of training data, rendering it a less complex task. Even a simpler model like Dense-CNN holds up well against DCRNN-based models without pretraining. Conversely, the classification task, a 4-class problem with imbalanced class distributions (Table 1), poses more challenges. The limited training samples for certain seizure types highlight the importance of multi-context correlations, illustrated by over 12% improvement in weighted F1 score by NeuroGNN without pretraining.

Table 3: Ablation study results, showing median performance over three trials and percentage changes relative to NeuroGNN. Bold and underline percentages highlight the largest and second-largest changes per metric.

	NeuroGNN	w/o. TemporalCorr	w/o. Semantics	w/o. Space	w/o. Meta-Nodes
Detection	**0.847**	0.831	0.828	0.818	0.829
(AUROC)	–	-2.12%	*-2.47%*	**-3.65%**	-2.36%
Classification	**0.790**	0.673	0.719	0.727	0.714
(Weighted F1)	–	**-14.81%**	-8.99%	-7.97%	*-9.62%*

Impact of Pretraining Consistent with findings in [30], our results validate the positive effect of pretraining on performance. Our specific pretraining task, aligned with NeuroGNN's design involving EEG nodes and meta-nodes representing brain regions, enhances performance, leading to a 3.42% boost in the AUROC metric for seizure detection. However, the increase in the weighted F1 score for classification is minor. This indicates that while pretraining aids in mitigating data scarcity and out-of-distribution challenges, the multi-context correlations captured by NeuroGNN intrinsically address these issues, making the benefits of pretraining less significant for NeuroGNN compared to DCRNN-based models. This reduction in pretraining necessity also implies a saving in computational resources and time, positioning NeuroGNN as a more resource-efficient and practical option for real-world applications.

4.3 Ablation Study

In this section, we explore the impact of NeuroGNN's individual components on performance by creating four distinct variants, each removing one aspect of the multi-context correlations. The variants are: (1) **W/O TemporalCorr:** NeuroGNN without temporal correlations for graph edge formation. (2) **W/O Semantics:** NeuroGNN without semantics in node features and graph edge weights. (3) **W/O Space:** NeuroGNN without spatial proximity information between nodes for graph edge formation. (4) **W/O Meta-Nodes:** NeuroGNN without aggregated time-series nodes representing brain regions.

We evaluated each variant on both seizure detection and classification tasks, with results presented in Table 3. As observed from the table, every component improves performance on both tasks. The ablation study shows a noticeable decrease in performance for the classification task in all configurations compared to the detection task. On average, the classification task experiences a 7.7% larger drop in performance in all configurations. This observation supports our claim that multi-context correlations significantly ease the challenges posed by data scarcity in rare classes and the complexity of multi-class classification. For example, the classification task has significantly fewer samples than the detection task (3,730 non-seizure and 869 seizure events), particularly for the AB and CT classes, which have only 50 and 48 training events, respectively.

The analysis indicates that spatial correlations have the most significant impact on the detection task, while temporal correlations affect classification performance the most, leading to a 3.65% and a substantial 14.81% drop in performance, respectively. This can be explained by the nature of the tasks. In seizure detection, the goal is to pinpoint the occurrence of seizures, which often relate

(a) Graph Embeddings from Dist-DCRNN   (b) Graph Embeddings from NeuroGNN
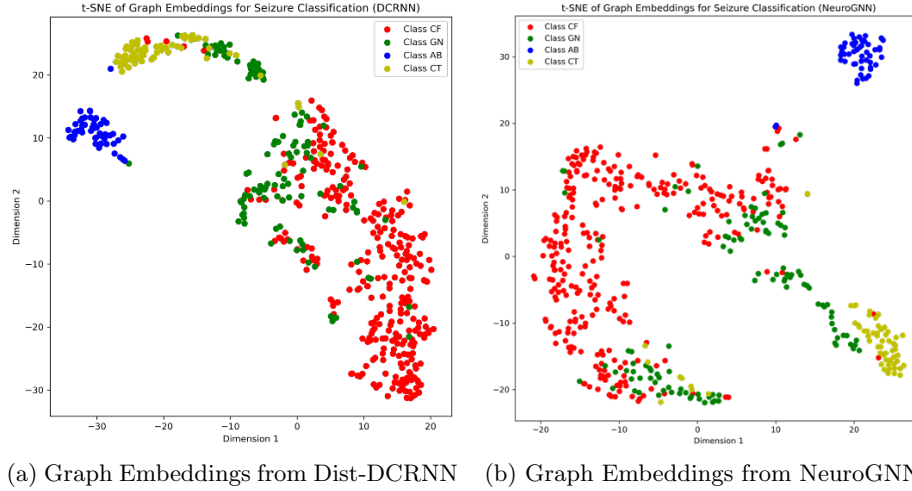
Fig. 3: Visualization of graph embeddings for seizure classification test samples using trained Dist-DCRNN and NeuroGNN models. The colors represent the ground truth seizure labels.

to unusual frequency patterns within a close neighborhood of EEG electrodes. On the other hand, classification requires a more detailed examination of frequency anomalies to distinguish the type of seizure, highlighting the importance of temporal relationships among different EEG electrodes and brain regions in associating an EEG clip with a specific seizure class.

4.4   Analysis of Graph Embeddings

This section explores the effectiveness of graph embeddings generated by pre-trained Dist-DCRNN and NeuroGNN on test samples for the classification task. The aim is to assess the effectiveness of the learned graph embeddings by NeuroGNN in comparison with the previous SOTA model in distinguishing different seizure types. After training on seizure classification, both models are used in inference mode to obtain graph embeddings for test samples, with initial weights set based on pretraining for a fair comparison.

The graph embeddings for the seizure classification test samples are visualized in a 2D space using the t-SNE dimensionality reduction technique [19] as depicted in Figure 3. These figures reveal a notable pattern of interleaving among samples of the GN seizure class and samples from other classes, which corresponds to a lower True Positive Rate for the GN seizure class, indicating higher classification difficulty for this particular seizure type.

The quality of embeddings is assessed quantitatively by clustering the original high-dimensional graph embeddings into four clusters using the KMeans algorithm, reflecting the number of classes in the dataset. The average clustering purity metric is computed to measure the homogeneity of clusters regarding class membership, defined as the mean of the maximum class proportion across

Table 4: F1 Score Comparison between NeuroGNN and Dist-DCRNN for Seizure Classification Across Different Training Data Ratios. "Improvement" shows the percentage improvement of NeuroGNN over Dist-DCRNN.

	Training Data Ratio				
	100%	80%	60%	40%	20%
Dist-DCRNN	0.701	0.704	0.679	0.689	0.606
NeuroGNN	0.790	0.795	0.772	0.787	0.781
Improvement	12.7%	12.9%	13.7%	14.2%	28.9%

all clusters. The analysis shows that NeuroGNN achieves an average clustering purity value of 0.747, compared to 0.717 for Dist-DCRNN, representing an 11% reduction in clustering impurity by NeuroGNN. This highlights NeuroGNN's superior ability to distinguish samples based on multi-context correlations.

4.5   Handling Scarce Training Data

Experiments were conducted to evaluate NeuroGNN and Dist-DCRNN's performance under different data availability scenarios by using subsampled versions of training data, while keeping the original class distribution through stratified sampling. The results, depicted in Table 4, show the median weighted F1 score in three independent runs for each sampling ratio in the training data, with evaluations performed on the entire test dataset to ensure consistency across all experiments.

The table illustrates that as the sampling ratio decreases, the performance gap between NeuroGNN and Dist-DCRNN increases, showcasing the robustness of NeuroGNN to smaller training sizes compared to Dist-DCRNN. Moreover, NeuroGNN's performance exhibits only slight degradation even with reduced training data, emphasizing the model's ability to effectively leverage multi-context correlations to address challenges posed by data scarcity, thereby maintaining a superior performance under data-constrained conditions.

5   Conclusion

We introduced NeuroGNN, a novel Graph Neural Network framework, to enhance seizure detection and classification from EEG data. While existing methods rely heavily on manual analysis or fail to capture the intricate brain dynamics, NeuroGNN dynamically integrates spatial, temporal, and semantic contexts. In our empirical evaluation, NeuroGNN consistently outperformed current state-of-the-art models, demonstrating its efficacy, especially when data is scarce for training, which is common when classifying rare seizures.

Acknowledgments

References

1. Ackerman, S., et al.: Discovering the brain (1992)
2. Ahmedt-Aristizabal, D., et al.: Neural memory networks for seizure type classification. In: IEEE EMBC (2020)
3. Asif, U., et al.: Seizurenet: Multi-spectral deep feature learning for seizure type classification. In: MLCN & RNO-AI Workshops at MICCAI (2020)
4. Bhattacharyya, A., et al.: Tunable-q wavelet transform based multiscale entropy measure for automated classification of epileptic eeg signals. Applied Sciences **7**(4), 385 (2017)
5. Chen, D., et al.: Measuring and relieving the over-smoothing problem for graph neural networks from the topological view. In: AAAI. vol. 34, pp. 3438–3445 (2020)
6. Falco-Walter, J.: Epilepsy—definition, classification, pathophysiology, and epidemiology. In: Seminars in neurology. vol. 40, pp. 617–623 (2020)
7. Glorot, X., Bengio, Y.: Understanding the difficulty of training deep feedforward neural networks. In: AISTATS. pp. 249–256 (2010)
8. Hajisafi, A., et al.: Learning dynamic graphs from all contextual information for accurate point-of-interest visit forecasting. arXiv preprint arXiv:2306.15927 (2023)
9. Hendrycks, D., et al.: Using pre-training can improve model robustness and uncertainty. In: ICML. pp. 2712–2721 (2019)
10. Hochreiter, S., Schmidhuber, J.: Long short-term memory. Neural Comput. **9**(8), 1735–1780 (1997)
11. Jiang, Y., et al.: Seizure classification from eeg signals using transfer learning, semi-supervised learning and tsk fuzzy system. IEEE Transactions on Neural Systems and Rehabilitation Engineering **25**(12), 2270–2284 (2017)
12. K. Cho, K., et al.: Learning phrase representations using rnn encoder-decoder for statistical machine translation. arXiv preprint arXiv:1406.1078 (2014)
13. Kingma, D.P., Ba, J.: Adam: A method for stochastic optimization. arXiv preprint arXiv:1412.6980 (2014)
14. Kipf, T.N., Welling, M.: Semi-supervised classification with graph convolutional networks. In: ICLR (2017)
15. Li, Y., et al.: Diffusion convolutional recurrent neural network: Data-driven traffic forecasting. In: ICLR (2018)
16. Lopez, S., et al.: Automated identification of abnormal adult eegs. In: Proc. IEEE SPMB. pp. 1–5 (2015)
17. Loshchilov, I., Hutter, F.: Sgdr: Stochastic gradient descent with warm restarts. arXiv preprint arXiv:1608.03983 (2016)
18. Ma, Y., et al.: Tsd: Transformers for seizure detection. bioRxiv pp. 2023–01 (2023)
19. van der Maaten, L., Hinton, G.: Visualizing data using t-sne. Journal of machine learning research **9**(11) (2008)
20. Obeid, I., Picone, J.: The temple university hospital eeg data corpus. Front. Neurosci. **10**, 196 (2016)
21. Roy, S., et al.: Deep learning enabled automatic abnormal eeg identification. In: Proc. IEEE EMBC. pp. 2756–2759 (2018)
22. Saab, K., et al.: Weak supervision as an efficient approach for automated seizure detection in electroencephalography. NPJ Digit. Med. **3**(1), 59 (2020)
23. Scrivener, C.L., Reader, A.T.: Variability of eeg electrode positions and their underlying brain regions: visualizing gel artifacts from a simultaneous eeg-fmri dataset. Brain and Behavior **12**(2), e2476 (2022)

24. Shah, V., et al.: The temple university hospital seizure detection corpus. Front. Neuroinform. **12**, 83 (2018)
25. Sharathappriyaa, V., et al.: Auto-encoder based automated epilepsy diagnosis. In: Proc. IEEE ICACCI. pp. 976–982 (2018)
26. Shoeibi, A., et al.: Epileptic seizures detection using deep learning techniques: A review. International Journal of Environmental Research and Public Health (2021)
27. Shuman, D., et al.: The emerging field of signal processing on graphs: Extending high-dimensional data analysis to networks and other irregular domains. IEEE signal processing magazine **30**(3), 83–98 (2013)
28. Song, K., et al.: Mpnet: Masked and permuted pre-training for language understanding. NeurIPS **33**, 16857–16867 (2020)
29. Strotzer, M.: One century of brain mapping using brodmann areas. Clinical Neuroradiology **19**(3), 179 (2009)
30. Tang, S., et al.: Self-supervised graph neural networks for improved electroencephalographic seizure analysis. In: Proc. of ICLR (2022)
31. Vaswani, A., et al.: Attention is all you need. NeurIPS **30** (2017)
32. Zeiler, M.D., Fergus, R.: Visualizing and understanding convolutional networks. In: ECCV. pp. 818–833 (2014)
33. Zilles, K.: Brodmann: a pioneer of human brain mapping—his impact on concepts of cortical organization. Brain **141**(11), 3262–3278 (2018)